Choosing the Best Rheological Model for Water-bentonite Suspensions

ROBERTO MAGLIONE
Consultant, Vercelli, Italy

VASSILIOS KELESSIDIS
Αναπληρωτής Καθηγητής Technical University of Crete, Mineral Resources Engineering Department

Abstract
Flow of water-bentonite dispersions is encountered in a variety of situations in oil-well drilling, chemical, petroleum and waste treatment industries and in complex geometries like pipe, concentric and eccentric annulus, and rectangular ducts. Most of the time, the flow of these dispersions is laminar and analytical solutions have been developed for a variety of rheological models like the Casson, the Robertson-Stiff, and the Herschel-Bulkley models. Couette viscometers are often used to determine the applicable rheological model but most of the time the shear rates experienced by the fluids are often computed as if the fluids were Newtonian or using a narrow gap approximation, giving thus only approximate values of the rheological parameters for the particular model. Recent advances, though, enable the computation of the true shear rates for any of the three models mentioned. Using Couette viscometric data from the literature, the three models are applied to obtain the rheological parameters using Newtonian and true shear rates in the narrow gap of the viscometer and the best fit model is determined. The flow parameters in laminar flow for pipes and annuli, such as velocity profile, pressure drop gradient as well as the onset of the transition to turbulent flow are then predicted. Differences in the rheological behaviour for all three models and from using Newtonian or true shear rates, as well as on the prediction of the flow parameters are evaluated and discussed.

1 INTRODUCTION

Water bentonite dispersions are used in many industries and in particular in oil-well drilling where they perform several important tasks for which determination of rheological properties is of primary importance. The shear stress – shear rate curves obtained with a Couette viscometer are most often characterized by non-linearity and exhibit yield stress (Bourgogne et al. 1991; Kelessidis et al. 2006; Kelessidis and Maglione 2006; Kelessidis et al. 2007; Kelessidis and Maglione 2008). Many rheological models have been suggested to describe the non-linear rheograms of these dispersions which relate shear stress t to shear rate $\dot{g}$, with three of them being of particular relevance to drilling fluid industry. These are, the three-parameter Herschel-Bulkley model (Herschel-Bulkley 1926; Fordham et al. 1991; Hemphil et al., 1993; Maglione and Ferrario 1996; Maglione et al. 2000; Kelessidis et al. 2005) given by

$$t = t_y + K\left(\dot{g}_{HB}\right)^n \quad \text{for } t \geq t_y \tag{1}$$

with t and $\dot{g}_{HB}$ are the yield stress and the shear rate of a Herschel-Bulkley fluid, K the flow consistency index and n the flow behaviour index; the three-parameter Robertson-Stiff model (Robertson and Stiff 1976; Beirute and Flumerfelt 1977)

$$t = A\left(\dot{g}_0 + \dot{g}\right)^m \quad \text{for } t \geq A\dot{g}_0^m \tag{2}$$

with A, $\dot{g}_0$, m the three rheological constants; and the two-parameter Casson model (Casson 1957; Bailey and Weir 1998)

$$\sqrt{t} = \sqrt{t_0} + \sqrt{m_p \dot{g}} \quad \text{for } t \geq t_0 \tag{3}$$

with t_0, m_p the Casson yield stress and the Casson plastic viscosity, respectively. Equations (1) and (3) state that there is no flow until a stress is developed which overcomes the yield stress, while equation (2) states that there is no yielding of the fluid until an initial strain is overcome.

The fluid rheograms ($t_i - \dot{g}_i$ data) are obtained using a variety of instruments. In oil-well drilling industry the instrument of choice is the narrow-gap Couette viscometer with a gap of 1.170 mm and a diameter ratio of 1.06780 (Bourgoyne et al. 1991; API 1993). Most of the time the shear rate values used in the reported rheograms are the values obtained assuming the fluid as Newtonian (by using the Newtonian shear rates, $\dot{g}_N$). If the fluid behaves according to one of the above mentioned models, the actual shear rates experienced by the fluid are different and depend on the particular model. This difference has been assessed for various rheological models by many investigators in the past (Krieger and Maron 1952, 1954; Krieger and Elrod 1953; Krieger 1968; Govier and Aziz 1972; Hanks 1983; Darby 1985; Joye 2003) using series

Submitted: Sept. 28 2009 Accepted: Oct 26 2010

expansion algorithms. It has been shown recently, though, that differences between the Newtonian shear rates and the true shear rates for Casson fluid, $\dot{\gamma}_C$, and for Robertson-Stiff fluid $\dot{\gamma}_{RS}$, albeit small, exist and should be taken into account (Kelessidis and Maglione 2006). Furthermore, the differences between Newtonian shear rates and Herschel-Bulkley fluid shear rates, $\dot{\gamma}_{HB}$, are even more significant (Kelessidis and Maglione 2008).

The choice of the best rheological model that characterizes water-bentonite dispersions is of extreme importance for computing pressure losses and velocity profiles, with the former contributing to oil-well safety (Bourgoyne et al. 1991) and the latter contributing to well cleaning from cuttings (Pilehvari et al. 1999; Kelessidis and Bandelis, 2004). The choice is normally done using non-linear regression with the best model giving the highest correlation coefficient R_c^2 but use of a linear regression correlation coefficient has been questioned for non-linear models (Helland 1988). Other statistical regression indicators have therefore been used such as the sum of square errors, SSE, and the root mean square error, RMSE (Maglione and Kelessidis 2006). In view of the fact that shear rates are also different for the different models, one has to wonder what would be the best fit rheological model of water-bentonite dispersions and whether evaluation of rheological parameters using Newtonian or true shear rates will have an effect on the particular choice. Similarly, the particular model chosen has an effect on the flow parameters of these dispersions, such as pressure loss and velocity profiles for flow in pipes and annuli, the typical geometries encountered in oil-well drilling.

It is, therefore, essential to be able to choose the best rheological model describing the rheological behaviour of these dispersions and to determine the consequences on the variables of interest, because the integration of rheological parameters with the hydraulic parameters is of special importance to drilling industry (Maglione et al. 1999). The flow of such yield-pseudoplastic fluids in various conduits such as pipes, annuli and ducts has been the subject of work of many investigators (Fordham et al., 1991; Van Pham and Mitsoulis, 1998; Bird et al., 2007; Mitsoulis 2007) but not taking into account elastic properties (Patil et al., 2008). The purpose of this paper is, hence, to analyze rheological data of water-bentonite dispersions reported in literature obtained with Couette viscometers, using Newtonian and true shear rates, and determine the best rheological model, among the three considered, using three statistical indicators. Then, the effect of using true versus Newtonian shear rates for the best chosen rheological model, for a suspension flowing in a pipe or an annulus, on pressure loss, velocity profiles and transition from laminar to turbulent flow is considered, using the models developed by Kelessidis et al. (2006) and Founargiotakis et al. (2008).

2 THEORY

For a Newtonian fluid, the shear stress, τ_i, developed on the inner cylinder of a narrow-gap viscometer with the outer cylinder rotating with a speed N_i revolutions per minute, is given by (Govier and Aziz 1972, Bird et al. 2007),

$$\tau_{Ni} = \frac{T}{2\pi r_i^2 L} = \left(\frac{2\delta^2}{\delta^2-1}\right)\left(\frac{2\pi N_i}{60}\right)(\mu) \quad (4)$$

where T is the torque developed on the stationary inner cylinder, r_i is the radius of the inner cylinder, L, is the cylinder length, δ, is the radius ratio of the viscometer ($\delta = 1.06780$ for narrow-gap viscometers used in oil-well drilling) (Bourgoyne et al. 1991), and μ is the Newtonian viscosity. Equation (4) gives the Newtonian shear rate, $\dot{\gamma}_{Ni}$, as,

$$\dot{\gamma}_{Ni} = \left(\frac{2\delta^2}{\delta^2-1}\right)\left(\frac{2\pi N_i}{60}\right) \quad (5)$$

The true shear rate in the narrow-gap viscometer for a Casson fluid, $\dot{\gamma}_{Ci}$, can be computed (Hanks 1983; Joye 2003; Kelessidis and Maglione 2006) as

$$\dot{\gamma}_{Ci} = \frac{1}{\mu_p}\left[\sqrt{\left(\frac{2\pi N_i}{60}\mu_p - \tau_0 \ln\delta\right)\frac{2\delta^2}{(\delta^2-1)} + \frac{4\delta^2\tau_0}{(\delta+1)^2}} + \sqrt{\tau_0}\left(\frac{\delta-1}{\delta+1}\right)\right]^2 \quad (6)$$

An equation for the true shear rate on the inner cylinder for a Robertson-Stiff fluid, $\dot{\gamma}_{RSi}$, has been suggested by Zaho (Maglione and Romagnoli 1999) and given in a final form as (Kelessidis and Maglione 2006)

$$\dot{\gamma}_{RSi} = \left(\frac{2\pi N_i}{60}\right)\left\{\frac{2\delta^{2/m}}{m(\delta^{2/m}-1)}\right\} + \dot{\gamma}_0\left[\frac{2\delta^{2/m}\ln\delta}{m(\delta^{2/m}-1)} - 1\right] \quad (7).$$

For Herschel-Bulkley fluids, the true shear rate, $\dot{\gamma}_{HBi}$, can be expressed as a series of j terms (Kelessidis and Maglione 2008). The flow problem becomes a mathematical inverse integral problem for which analytical solution has not been found and in order to derive the series expansion solution, two cases must be considered (Kelessidis and Maglione 2008): for $\tau_i \le 2\tau_y$, which is usually true for values of rotational speed between 3 and 6 rpm, the true shear rate can be given by,

$$\dot{\gamma}_{HB} = \left\{ \frac{\tau_i}{K} - \left[\frac{2\left(\frac{2\pi N_i}{60}\right)}{\sum_{j=0}^{\infty} (-1)^j \left[\frac{\left(\frac{\tau_i}{\tau_y}-1\right)^{1/n+1+j} - \left(\frac{\tau_i}{\tau_y \delta^2}-1\right)^{1/n+1+j}}{1/n+1+j}\right]}\right]^n \right\}^{1/n} \quad (8)$$

For $\tau_i > 2\tau_y$, normally satisfied for rotational speeds greater than 6 rpm, the true shear rate is given by,

$$\dot{\gamma}_{HB} = \left\{ \frac{\tau_i}{K} - \left[\frac{2\left(\frac{2\pi N_i}{60}\right)}{\sum_{j=0}^{\infty} (-1)^j \left[\frac{\left(\frac{\tau_i}{\tau_y}-1\right)^{1/n-j} - \left(\frac{\tau_i}{\tau_y \delta^2}-1\right)^{1/n-j}}{1/n-j}\right]}\right]^n \right\}^{1/n} \quad (9).$$

The sum of square errors, SSE, and the root mean square error, $RMSE$, can be computed for any of the suggested models by,

$$SSE = \sum_{i}^{N_m} \left(\tau_i - \hat{\tau}_i\right)^2 \quad (10)$$

$$RMSE = \sqrt{\frac{SSE}{N_m - p}} \quad (11)$$

where $\hat{\tau}_i$ is the predicted shear stress value, N_m is the number of measurements and p are the degrees of freedom (the number of parameters in the rheological model), which for the Casson model is two and for the RS and the HB models is three.

In order to compute the effects of different approaches on pressure loss estimation, these are estimated for a series of flow rates covering laminar flow of such fluids in pipes and annulus as well as the onset of transition to turbulent flow for these geometries, as these are dependent strongly on the values of the rheological parameters. The procedure followed to predict the onset of laminar to transitional flow regime was developed by Founargiotakis et al. (2008). To this end, the flow equation for laminar flow is analytically solved using the Kelessidis et al. (2006) approach. For transition to turbulent flow, defined by the Reynolds number where departure from laminar flow friction factor data is observed (Dodge and Metzner 1959), use of the local power-law assumption is made, as follows,

$$\tau_w = K'\left(\dot{\gamma}_{Nw}\right)^{n'} \quad (12)$$

The expressions of the local-power law parameters were provided by Founargiotakis et al. as,

$$n' = \frac{n(1-\xi)(n\xi + n + 1)}{1 + n + 2n\xi + 2n^2\xi^2} \quad (13)$$

and

$$K' = \frac{\tau_y + K\left(\frac{2n'+1}{3n'}\dot{\gamma}_{Nw}\right)^n}{\left(\dot{\gamma}_{Nw}\right)^{n'}} \quad (14).$$

and

$$\xi = \frac{\tau_y}{\tau_w} \quad (15)$$

The values of Newtonian shear rates, $\dot{\gamma}_{Nw}$, are given, for circular conduits by,

$$\dot{\gamma}_{Nw} = \frac{8V}{d} \quad (16)$$

and for concentric annuli, which is considered as a slot, by,

$$\dot{\gamma}_{Nw} = \frac{12V}{\left(d_o - d_i\right)} \quad (17)$$

Onset of transition from laminar to ttransitional flow occurs at values of the modified Reynolds number which are function of n', taken from the Dodge and Metzner (1959) graph as,

$$\mathrm{Re}_1 = 3250 - 1150(n') \quad (18)$$

where the generalized Reynolds number for the flow of Herschel-Bulkley fluid, with $\mu_e = \tau / \dot{\gamma}_w$, in an annulus becomes,

$$\mathrm{Re}_{MRa} = \frac{\mathrm{r}\, V(d_2 - d_1)}{\mathrm{m}_e} = \frac{\mathrm{r}\, V^{2-n'}(d_2 - d_1)^{n'}}{K'(12)^{n'-1}} \qquad (19).$$

while in a pipe becomes,

$$\mathrm{Re}_{MRp} = \frac{\mathrm{r}\, V^{2-n'} d^{n'}}{K'(8)^{n'-1}} \qquad (20).$$

Thus, the transition points are not fixed but they are function of fluid rheology, flow rate and conduit diameters thus requiring iteration, where one assumes that flow is laminar or transitional, and solves the system, with the ultimate check that the calculated flow rate matches the given flow rate.

3 MATERIALS AND METHODS

Rheological data from four water-bentonite dispersions, taken from the literature (Kelessidis et al. 2005), samples S1, S2, S5, and S7, at different bentonite concentrations and densities ranging from 1,050 and 1,080 kg/m^3, have been analyzed to determine which amongst the Casson, the Robertson-Stiff (RS), and the Herschel-Bulkley (HB) models fitted better the raw experimental data. The sets of experimental data were taken with a Grace M3500a Couette viscometer, with an inner cylinder radius of 1.7245 cm, an outer cylinder radius of 1.8415 cm, and cylinder length of 3.80 cm. Preparations and mixing procedures were carried out according to API 13A guidelines (API 1993). The dispersions were left for 16 hours for complete hydration of bentonite particles, and then agitated vigorously for 5 minutes before making viscometer measurements. Rheological data is listed in Table 1.

Non-linear regression was performed on the raw experimental data sets ($\mathrm{t}_i - \mathrm{N}_i$) using standard non-linear regression packages to fit the Casson, RS and HB model equations by first assuming that shear rates in the gap of the viscometer are Newtonian, given by Eqn. (5), and the appropriate rheological parameters for each model were then determined. Non-linear regression to the experimental data set was also performed, to determine the rheological parameters also with the use of the Casson and Robertson-Stiff true shear rate equations, given by equations 6 and 7, respectively. The rheological parameters using Herschel-Bulkley true shear rates, equations 8 and 9, were determined using a numerical algorithm presented before (Kelessidis and Maglione 2008). Following the evaluation of the rheological parameters, the three statistical indicators were then estimated, the correlation coefficient, R_c^2, the sum of square errors, , and the root mean square error, .

The appropriate rheological model, either using the Newtonian shear rate or the true shear rate, was chosen as the best fit of the rheograms to the raw experimental data according to the statistical correlation parameters. Differences in the prediction of flow parameters in laminar flow by using the best fit model, both in pipes and annuli, such as velocity profiles, pressure drop gradient, and onset of the transitional flow regime when using Newtonian and true shear rates were then evaluated.

4 RESULTS AND DISCUSSION

Figure 1 shows the behavior of the experimentally-derived and computed Newtonian shear rates-based rheograms for sample S1. Table 2 reports the rheological parameters that characterize the three rheological models related to the four bentonite dispersions as well as the statistical coefficients R_c^2, SSE and $RMSE$, for the case of using Newtonian shear rates. As it can be seen from all three statistical indicators, the HB model exhibits the best fit of the raw experimental data in two out of the four cases (samples S1 and S2) while for samples S5 and S7, the best fit is observed for the Casson and for the RS model, respectively, but the HB model exhibits very close values of these indices to those from the other models.

Figure 2 shows the comparison of the experimentally derived and computed true shear rate-based rheograms for sample S1. Table 3 reports the true rheological parameters that characterize the three models as well as the related statistical correlation coefficients. It can be seen from the reported tables that in the case of using true shear rates, the HB model exhibits the best fit of the experimental data in three cases (S1, S5 and S7) while for the sample S2 data the RS model gives the best fit, although HB model performs equally well.

Figure 3 shows the ratio of the true shear rate to the Newtonian shear rate for each model for sample S1. The lines connecting the points reported on Figure 3 are drawn with the purpose to give a more immediate overall view to the trend of the ratios. For shear rates greater than 200 s^{-1}, the computed Newtonian shear rates are higher than the true shear rates, for all three rheological models, with the ratio floating around 1.20, and at lower shear rates, Newtonian shear rates are much higher than true shear rates, with the ratios ranging between 1.5 to 3.5 for all rheological models. A similar behaviour was also observed for samples S2, S5, and S7, not shown here for brevity. Thus, assumption of Newtonian shear rates leads to higher values than those by using the true shear rates which results in predicting larger rheological parameters for all tested models.

The oscillations observed of the ratio of the true shear rate to the Newtonian shear rate for the HB model might be the consequence of the irregular trend of the experimental data set, above all at low shear rates. Oscillations for the same ratio, though smoother, were also observed on the S2, S5, and S7 samples. This behaviour might be also attributed to calculation noise in the procedure to determine the true shear rate that may occur with a different weight for different experimental data set.

The above comparison indicated that the HB model based on true shear rates is the best rheological model, amongst the three considered models, to describe the rheological viscometer data set. Use then of the HB rheological parameters was done to determine the effect on the flow parameters.

Figure 4 shows the velocity profiles for laminar flow in a pipe, with internal diameter (ID) of 0.1085 m (4.27-in), at 500 L/min and 1,000 L/min (132 and 264 gpm) predicted by the HB model for sample S1. Computations were performed with the Kelessidis et al. (2006) model using rheological parameters derived with the Newtonian shear rate and the true shear rate. In Figure 5 the velocity profiles in a (0.2159 m by 0.127 m – 8.5 by 5.0-in) annulus at 750 L/min and 1,500 L/min (198 and 397 gpm) predicted by the HB model are also reported for both shear rates for Sample 7. Figure 4 and 5 show small differences amongst the velocity profiles of the water-bentonite dispersions computed by the HB model derived either by the Newtonian or the true shear rate, with the plug width being larger when using Newtonian shear rate derived rheological parameters.

Tables 4 and 5 report the plug flow region related to the HB model derived by either Newtonian or true shear rate, for samples S1 and S7, and for each pump rate. It can be seen from the values of the radii R_{1max} and $R_{2max,}$ respectively the onset and the end of the plug flow region, a relatively high reduction (with values as low as -55.1%) of the extension of the plug flow when the velocity profile is calculated by making resort to the HB true shear rate.

In Figures 6 through 8 results are reported for the predicted pressure drop gradient in laminar flow regime in the same pipe for the HB model derived by Newtonian shear rate and by true shear rate for the samples S1, S7, and S5, respectively. The results show that the pressure drop gradient calculated with rheological parameters derived using the true shear rates is all the time lower than the corresponding one computed with rheological parameters determined using the Newtonian shear rates. The maximum differences range around (–8.7%) for sample S1, (-7.4%) for sample S2, (–19.1%) for sample S5 and (-15.9%) for sample S7, noting also that as the flow rate is increased these differences become a bit smaller. Differences on the onset of the predicted transitional flow regime is also anticipated when the simulation is performed using the HB rheological parameters derived by the true shear rates. The largest difference was found for sample S5, where the prediction of the onset of the transitional flow was at 481 L/min (127 gpm), when computed by the Newtonian shear rate, and at 436 L/min (115 gpm), when calculated by the true shear rates.

Figures 9 and 10 show the pressure drop gradient in the same annulus as above, in laminar flow regime for the HB model, with rheological parameters derived by Newtonian shear rate and true shear rate, for samples S7 and S5, respectively. The results show that, as in the case for flow in pipes, the pressure drop gradient calculated with rheological parameters estimated using true shear rates is always smaller than the corresponding ones computed with rheological parameters estimated using Newtonian shear rates, with differences ranging from (–18.0%) for sample S5 to (–13.3%) for sample S7. In addition, the onset of the transitional flow regime is different, with the largest difference found for sample S5, where onset of the transitional flow was predicted at 1,163 L/min (308 gpm), when computed with rheological parameters estimated by using the Newtonian shear rate, and 1,077 L/min (285 gpm), when calculated with rheological parameters estimated by using the true shear rate.

Figure 11 shows the ratio of the computed critical flow rates for the onset of the transition from laminar to transitional flow regime, in pipe and in annulus, derived with rheological parameters estimated using the true shear rate and the Newtonian shear rate, for the four analysed samples. It is evident that in all the cases considered for both pipe and annuli, the ratio of the critical flow rates is below 1.0 and ranges between 0.91 and 0.97 with sample S5 showing the smallest ratio.

5 CONCLUSION

Rheological experimental data of water-bentonite dispersions have been analysed to determine whether they can be described by Casson, Robertson-Stiff, or Herschel-Bulkley model. Equations have been used which allow the determination of the true shear rate experienced by the fluid in the gap of a Couette viscometer when using any of the three rheological models. This allowed the determination of the rheological parameters for all three models using both true and Newtonian shear rates.

Differences were observed between the rheological parameters computed by applying either the Newtonian or the true shear rate expressions for all tested models. The three-constant parameters of the Herschel–Bulkley rheological model computed using the true shear rates gave the best fit to the experimental data for all tested samples while computation with Casson model gave the lowest accuracy.

For flow of water-bentonite dispersions in pipe and annulus, using the best fit rheological model (Herschel-Bulkley model), differences were observed between the computed flow parameters using the rheological parameters derived with Newtonian shear rates versus those determined with true shear rates. Up to (-19.1%) differences have been estimated for the pressure drop gradient, indicating that with current normal practice, errors in estimation of energy losses are of the same amount. On the other hand, only small differences have been found for the velocities profiles, both in pipes and annuli, indicating that cuttings transport is not jeopardized using current practices. Variations in the critical flow rates for the onset of transitional flow from laminar to turbulent flow in pipes and annuli, have also been observed which ranged between (-9.0%) and (-7.0%) respectively for the fluids tested.

REFERENCES

American Petroleum Institute Specifications 13A (1993) Specification for Drilling Fluids Materials

Bailey WJ, Weir IS (1998) Investigation of methods for direct rheological model parameter estimation. J Petrol Science and Engineering 21:1-13

Beirute RM, Flumerfelt RW (1977) An evaluation of the Robertson-Stiff model describing rheological properties of drilling fluids and cement slurries. Soc Petr Engrs J 17:97-100

Bird, RB, Stewart WE and Lightfoot EN (2007) Transport Phenomena (Revised Second Edition ed.). John Wiley & Sons

Bourgogne AT, Chenevert ME, Millheim KK, Young FS (1991) Applied Drilling Engineering, vol 2. SPE Textobook Series, Richardson

Casson N (1957) A flow equation for pigment-oil dispersions of the printing ink type, in Mill CC (edts) Rheology of disperse systems. Proceedings of the Conference of the British Society of Rheology, University College, Swansea, Pergamon, London

Darby R (1985) Couette viscometer data reduction for materials with a yield stress. J Rheol 29:369-378

Dodge DW, Metzner AB (1959) Turbulent flow in non-Newtonian systems. AIChE J. 5:189–204

Fordham EJ, Bittleston SH, Tehrani MA (1991) Viscoplastic flow in centered annuli, pipes and slots. I & EC Research 29:517-524

Founargiotakis K, Kelessidis VC, Maglione R (2008) Laminar, turbulent and transitional flows of Herschel-Bulkley fluids in annuli, Can. J. Chem. Eng., 86:676-683.

Govier GW, Aziz K (1972) The flow of complex mixtures in pipes. Krieger, Malabar, Florida, USA.

Hanks RW (1983) Couette viscometry of Casson fluids. J Rheol 27:1-6.

Helland I (1988) On the structure of partial least squares regression. Communications in Statistics-Simulation and Computations 17:581-607

Hemphil T, Campos W, Tehrani MA (1993) Yield power law model accurately predicts mud rheology. Oil Gas J. 91, 45–50.

Herschel WH, Bulkley R (1926) Konsistenzmessungen von Gummi-Benzollosungen. Kolloid Z 39:291–300.

Joye DD (2003) Shear rate and viscosity corrections for a Casson fluid in cylindrical (Couette) geometries. J Colloidal and Interface Sci 267:204-210

Kelessidis VC, Bandelis GE (2004) Flow patterns and minimum dispersion velocity for efficient cuttings transport in horizontal and deviated wells in coiled–tubing drilling. SPE Drilling and Completion 19:213-227

Kelessidis VC, Mihalakis TS, Tsamantaki C (2005) Rheology and rheological parameter determination of bentonite–water and bentonite–lignite–water mixtures at low and high temperatures. Proceedings 7th World Congress in Chem. Engineering, Glasgow, July 2005.

Kelessidis VC, Maglione R (2006) Modeling rheological behavior of bentonite suspensions as Casson and Robertson-Stiff fluids using Newtonian and true shear rates in Couette viscometry, Powder Tech 168, 137-147.

Kelessidis VC, Maglione R, Tsamantaki C, Aspirtakis, Y (2006) Optimal determination of rheological parameters for Herschel-Bulkley drilling fluids and impact on pressure drop, velocity profiles and penetration rates during drilling, J. Petr. Science & Eng. 53, 203-224.

Kelessidis VC, Tsamantaki C, Dalamarinis P (2007) Effect of pH and electrolyte on the rheology of aqueous Wyoming bentonite dispersions, Appl. Clay Sci, 38, 86–96.

Kelessidis VC, Maglione R (2008) Shear rates corrections for Herschel-Bulkley fluids in Couette geometry and effects on frictional loss estimation, Appl. Rheol. 18:3, 34482-1 – 34482-11

Krieger IM (1968) Shear rate in the Couette viscometer. Trans Soc Rheology 12:5-11

Krieger IM, Maron SH (1952) Direct determination of flow curves of non-Newtonian fluids. J Applied Physics 23:147-149

Krieger IM, Elrod H (1953) Direct determination of flow curves of non-Newtonian fluids. J Applied Physics 24:134-137.

Krieger IM, Maron SH (1954) Direct determination of the flow curves of non-Newtonian fluids, III Standardized treatment of viscometric data. J Applied Physics 25:72-76.

Maglione R, Robotti G (1996) A Numerical Procedure for Solving a N non-Linear Equations Systems for Determining the Three Rheological Parameters of a Drilling Mud from Experimental Data. Proceeding of the Fourth International Conference on Integral Methods in Science and Engineering, pp 144-149.

Maglione R, Ferrario G (1996) Equations determine flow states for yield-pseudoplastic drilling fluids. Oil Gas J. 94, 63–66.

Maglione R, Romagnoli R (1999) Idraulica dei Fluidi di Perforazione. Edizioni Cusl, Turin (Italy).

Maglione R, Guarneri A, Ferrari G (1999) Rheologic and hydraulic parameter integration improves drilling operations. Oil Gas J. 97, 44–48.

Maglione R, Robotti G, Romagnoli R (2000) In-situ characterization of drilling mud. SPE Journal 5:377-386.

Maglione R., Kelessidis VC (2006), Choosing the best rheological model for bentonite suspensions, Proceedings, 3rd Annual European Rheology Conference, Hersonissos Crete, April 27-29.

Mitsoulis E (2007) Flows of Viscoplastic Materials: Models and Computations, Rheology Reviews, London, UK, Brit. Soc. Rheol., 135-178 pages (bookchapter).

Patil PD, Ochoa I, Feng JJ and Hatzikiriakos SG (2008), Viscoelastic flow simulation of polytetrafluoroethylene (PTFE) paste extrusion, J Non-Newtonian Fluid Mechanics, 153:25-33

Pilehvari AA, Azar JJ, Shirazi SA (1999) State of the art cuttings transport in horizontal wellbores. SPE Dril and Compl 14: 196–200

Robertson RE, Stiff HA (1976) An improved rheological model for relating shear stress to shear rate in drilling fluids and cement slurries. Soc Pet Engrs J 16:31-36.

Van Pham T, Mitsoulis E (1998) Viscoplastic flows in ducts, The Canadian Journal of Chemical Engineering, 76:120–125.

Table 1 *Rheological data of the samples used* [a]

Πίνακας 1. *Ρεολογικά δεδομένα για τα δείγματα που χρησιμοποιήθηκαν*

RPM	S1 - τ_i, Pa	S2 - τ_i, Pa	S5 - τ_i, Pa	S7 - τ_i, Pa
600	28.50	48.42	10.25	18.17
500	27.75	46.83	8.92	16.67
400	26.83	44.58	7.83	14.75
300	25.00	41.58	5.92	12.75
200	22.58	37.83	4.75	9.92
100	21.00	35.67	3.42	6.50
80	21.00	33.25	3.08	6.17
60	20.08	30.83	2.92	5.75
30	16.67	27.42	2.00	4.00
20	17.50	27.83	1.67	4.17
10	16.00	21.90	1.25	3.33
6	14.67	23.75	1.00	3.25
3	13.20	19.90	0.50	2.80

[a]from Kelessidis et al. (2005); 6.42% Zenith bentonite-water dispersions.

Table 2 *Rheological parameters derived by Newtonian shear rate and statistical correlation coefficients for all samples*
Πίνακας 2. *Ρεολογικές παράμετροι που ελήφθησαν με χρήση Νευτώνειων ρυθμών διάτμησης και οι στατιστικοί δείκτες*

	S1			**S2**			**S5**			**S7**		
	Casson	*R-S*	*H-B*	*Casson*	*R-S*	*H-B*	*Casson*	*R-S*	*H-B*	*Casson*	*R-S*	*H-B*
τ_0, τ_y [Pa]	14.540	-	8.475	22.00	-	9.807	0.710	-	0.675	2.173	-	2.3965
μ_p, K, A [Pa·s^n]	0.0026	9.209	3.401	0.0057	13.08	6.918	0.0054	0.112	0.073	0.0080	0.261	0.127
$\dot{\gamma}_0$ [1/s]	-	6.499	-	-	6.184		-	21.2	-	-	47.360	-
n, m	-	0.162	0.256	-	0.188	0.247	-	0.646	0.700	-	0.611	0.699
R_c^2	0.955	0.986	0.988	0.955	0.988	0.996	0.994	0.993	0.9937	0.9970	0.9980	0.9978
SSE [Pa^2]	14.090	4.486	3.877	50.040	13.480	12.840	0.719	0.910	0.800	1.260	0.760	0.919
RMSE [Pa]	1.132	0.670	0.623	2.133	1.167	1.133	0.256	0.302	0.283	0.338	0.276	0.303

Table 3 *Rheological parameters derived by true shear rates and statistical correlation coefficients for all samples*

Πίνακας 3. *Ρεολογικές παράμετροι που ελήφθησαν με χρήση πραγματικών ρυθμών διάτμησης και οι στατιστικοί δείκτες*

	S1			**S2**			**S5**			**S7**		
	Casson	*R-S*	*H-B*	*Casson*	*R-S*	*H-B*	*Casson*	*R-S*	*H-B*	*Casson*	*R-S*	*H-B*
τ_0, τ_y [Pa]	13.670	-	5.970	20.770	-	9.030	0.666	-	0.410	2.039	-	1.46
μ_p, K, A [Pa·s^n]	0.0026	8.754	4.140	0.0056	12.44	6.166	0.0054	0.11	0.08	0.0079	0.255	0.225
$\dot{\gamma}_0$ [1/s]	-	6.090	-	-	5.79	-	-	19.86	-	-	44.380	-
n, m	-	0.162	0.236	-	0.188	0.259	-	0.646	0.690	-	0.611	0.619
R_c^2	0.9580	0.986	-	0.956	0.976	-	0.994	0.993	-	0.9970	0.9980	-
SSE [Pa^2]	13.217	4.489	2.420	48.14	13.48	14.74	0.718	0.910	0.299	1.26	0.760	0.635
RMSE [Pa]	1.096	0.670	0.469	2.092	1.16	1.214	0.255	0.302	0.173	0.338	0.276	0.252

Table 4 *Plug flow region extension computed by the HB model rheological parameters derived by either the Newtonian or the true shear rate for sample S1*

Πίνακας 4. *Ορισμός περιοχής ροής εμβόλου με υπολογισμό HB μοντέλου με χρήση Νευτώνειων και πραγματικών ρυθμών διάτμησης για το δείγμα S1.*

	Sample S1			
	Q = 500 L/min		Q = 1000 L/min	
	HB-Ne shear rate	HB -True shear rate	HB-Ne shear rate	HB-True shear rate
Plug flow $R_{1,max}$ [m]	0.0343	0.0435	0.0363	0.0448
Plug flow $R_{2,max}$ [m]	0.0741	0.065	0.0721	0.0637
Difference [%]	-	- 46.0	-	-47.2

Table 5 *Plug flow region extension computed by the HB model rheological parameters derived by either the Newtonian or the true shear rate for sample S7*

Πίνακας 5. *Ορισμός περιοχής ροής εμβόλου με υπολογισμό HB μοντέλου με χρήση Νευτώνειων και πραγματικών ρυθμών διάτμησης για το δείγμα S7.*

	Sample S7			
	Q = 750 L/min		Q = 1500 L/min	
	HB-Ne shear rate	HB-True shear rate	HB-Ne shear rate	HB-True shear rate
Plug flow $R_{1,max}$ [m]	0.0770	0.0815	0.0789	0.0827
Plug flow $R_{2,max}$ [m]	0.0944	0.0900	0.0925	0.0888
Difference [%]	-	-51.1	-	-55.1

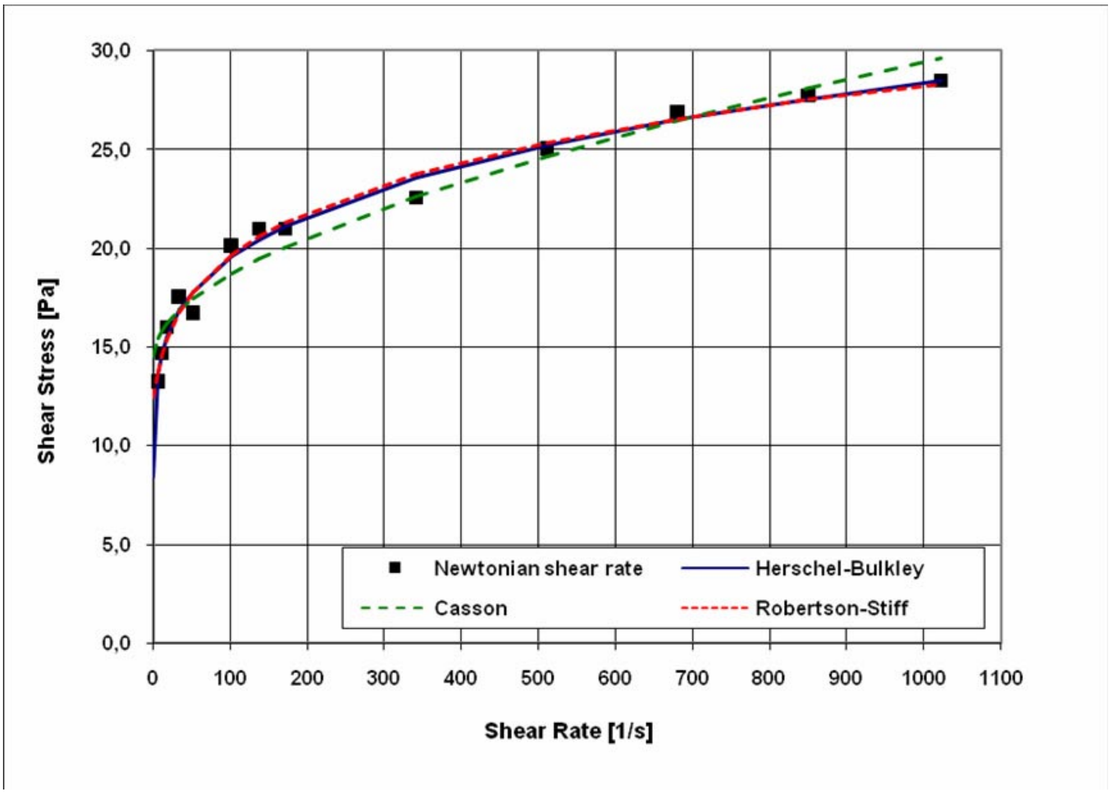

Fig. 1 *Experimentally-derived and computed Newtonian shear rate-based rheograms for sample S1*

Σχήμα 1. Ρεογράμματα από τα πραγματικά δεδομένα και εκτιμηθέντα με χρήση Νευτώνειων ρυθμών διάτμησης για το δείγμα S1.

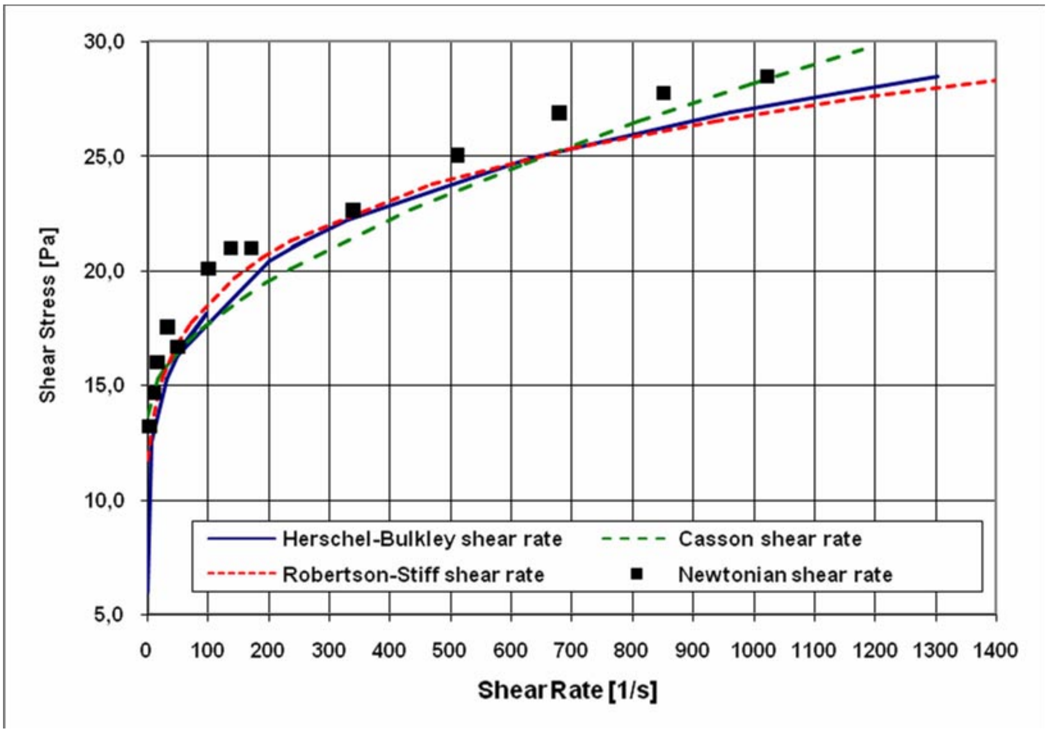

Fig. 2 *Experimentally-derived and computed true shear rate-based rheograms for sample S1*

Σχήμα 2. Ρεογράμματα από τα πραγματικά δεδομένα και εκτιμηθέντα με χρήση πραγματικών ρυθμών διάτμησης για το δείγμα S1.

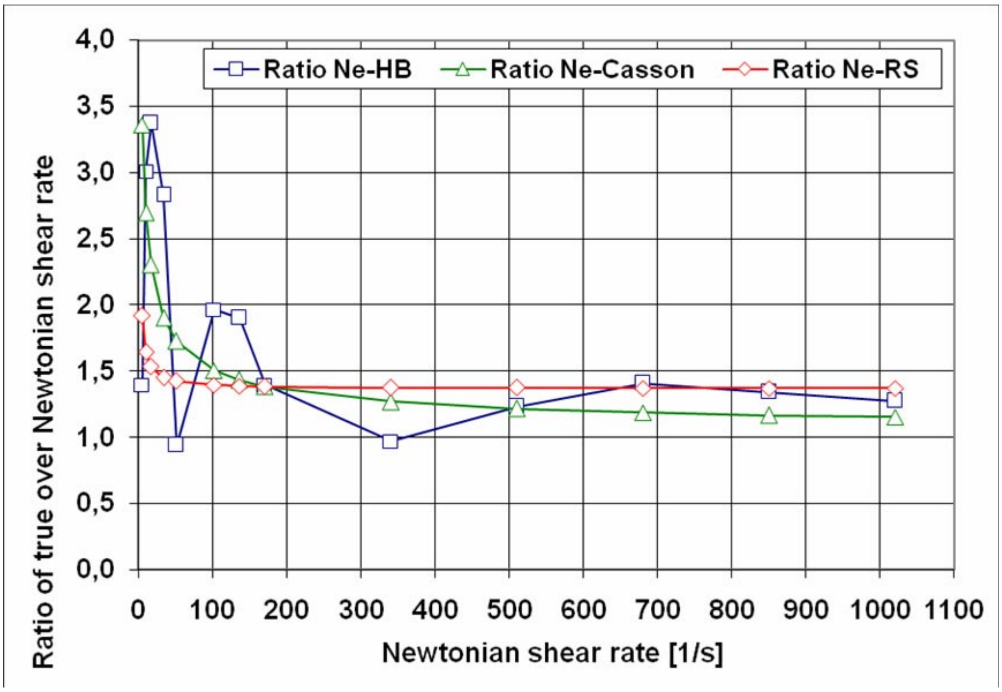

Fig. 3 *Ratio of true to Newtonian shear rate for sample S1*

Σχήμα 3. Λόγοι πραγματικών προς Νευτώνειων ρυθμών διάτμησης για το δείγμα S1.

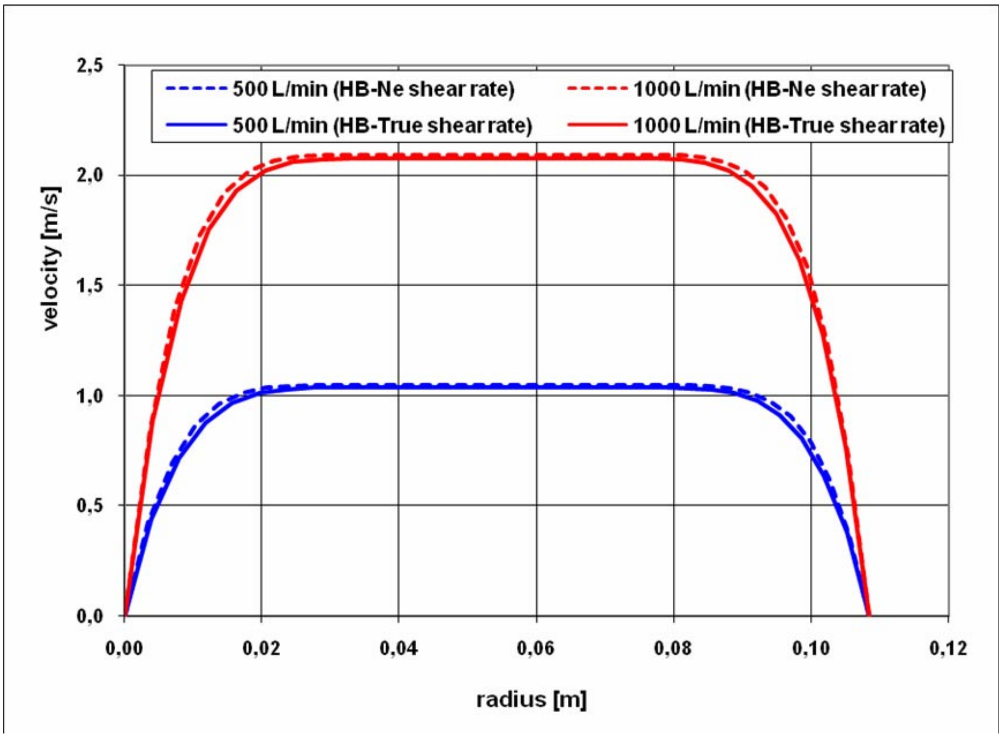

Fig. 4 *Predicted velocity profiles in pipe (ID=0.1085 m) in laminar flow for HB model rheological parameters derived by Newtonian and true shear rate for sample S1*

Σχήμα 4. Εκτιμώμενα προφίλ ταχύτητας για σωλήνα (ID=0.1085 m) σε στρωτή ροή για μοντέλο HB, με χρήση πραγματικών και Νευτώνειων ρυθμών διάτμησης, για το δείγμα S1.

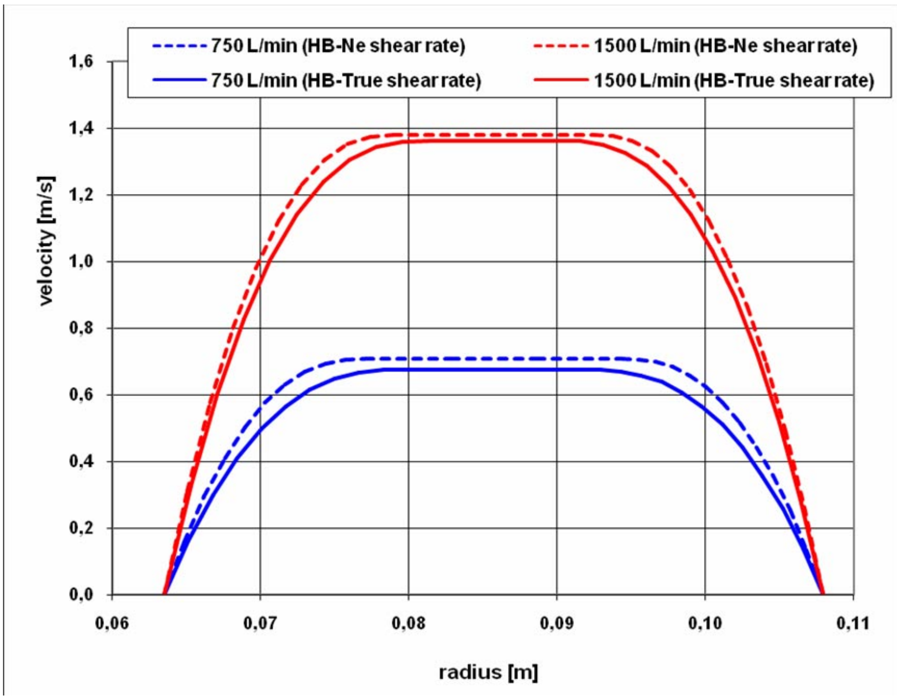

Fig. 5 *Predicted velocity profiles in annulus (0.2159 x 0.127 m) in laminar flow for HB model rheological parameters derived by Newtonian and true shear rate for sample S7*

Σχήμα 5. Εκτιμώμενα προφίλ ταχύτητας για δακτύλιο (0.2159 x 0.127 m) σε στρωτή ροή για μοντέλο HB, με χρήση πραγματικών και Νευτώνειων ρυθμών διάτμησης, για το δείγμα S7.

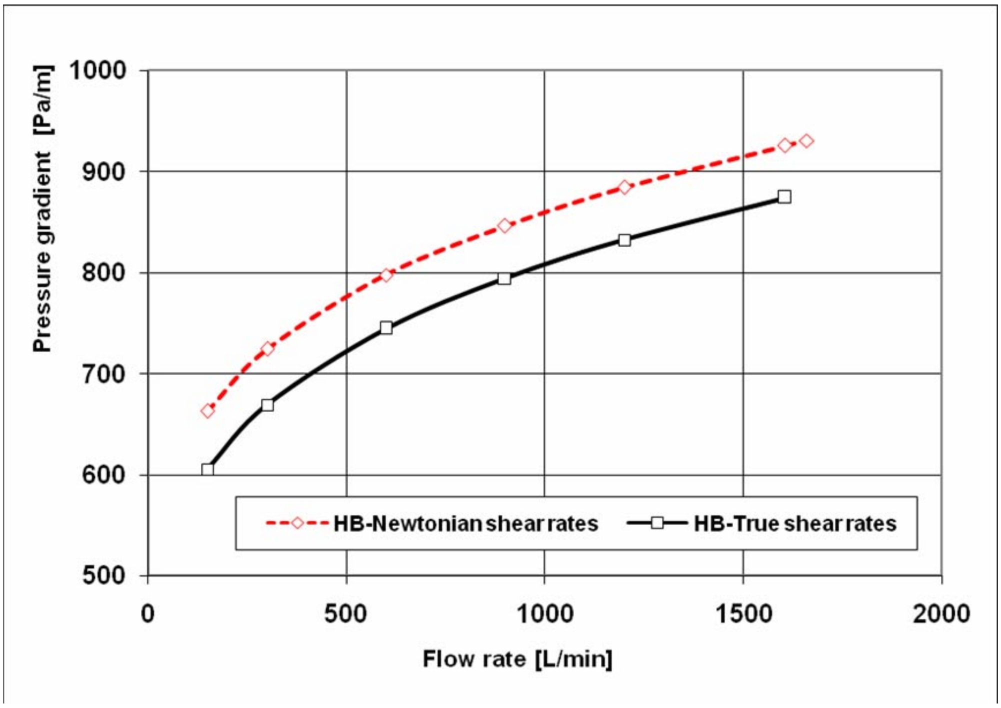

Fig. 6 *Predicted pressure drop gradient in pipe (ID=0.1085 m) in laminar flow regime, for HB model rheological parameters derived by Newtonian and true shear rate for sample S1*

Σχήμα 6. Εκτιμώμενη πτώση πίεσης για σωλήνα (ID=0.1085 m) σε στρωτή ροή για μοντέλο HB, με χρήση πραγματικών και Νευτώνειων ρυθμών διάτμησης, για το δείγμα S1.

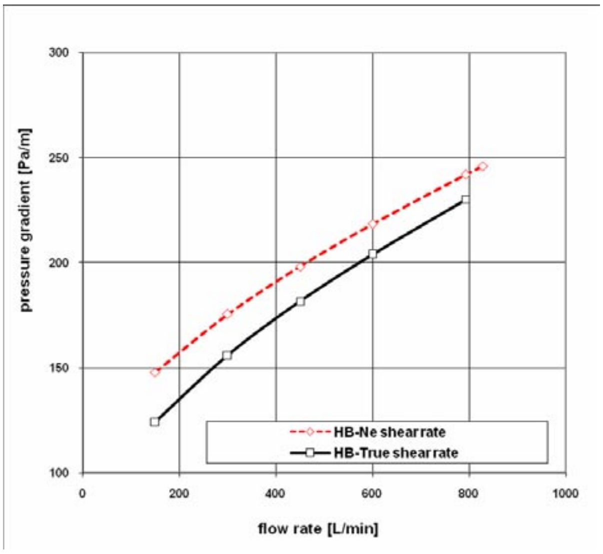

Fig. 7 *Predicted pressure drop gradient in pipe (ID=0.1085 m) in laminar flow regime, for HB model rheological parameters derived by Newtonian and true shear rate for sample S7*

Σχήμα 7. Εκτιμώμενη πτώση πίεσης για σωλήνα (ID=0.1085 m) σε στρωτή ροή για μοντέλο HB, με χρήση πραγματικών και Νευτώνειων ρυθμών διάτμησης, για το δείγμα S7.

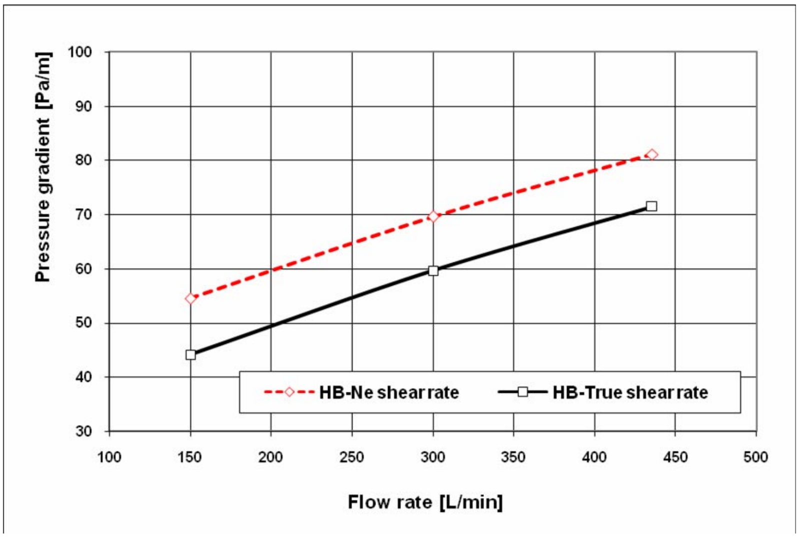

Fig. 8 *Predicted pressure drop gradient in pipe (ID=0.1085 m) in laminar flow regime, for HB model rheological parameters derived by Newtonian and true shear rate for sample S5*

Σχήμα 8. Εκτιμώμενη πτώση πίεσης για σωλήνα (ID=0.1085 m) σε στρωτή ροή για μοντέλο HB, με χρήση πραγματικών και Νευτώνειων ρυθμών διάτμησης, για το δείγμα S5.

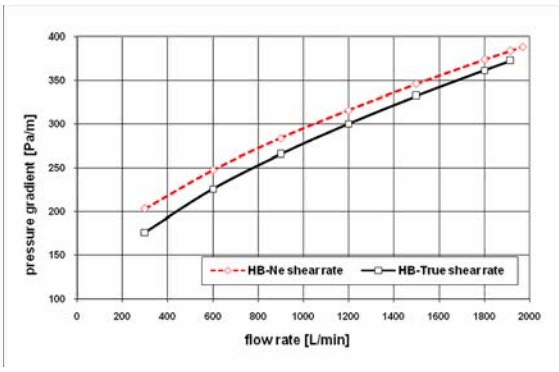

Fig. 9 *Predicted pressure drop gradient in (0.2159 by 0.127 m) annulus in laminar flow regime, for HB model rheological parameters derived by Newtonian and true shear rate for sample S7*

Σχήμα 9. Εκτιμώμενη πτώση πίεσης για δακτύλιο (0.2159 X 0.127 m) σε στρωτή ροή για μοντέλο HB, με χρήση πραγματικών και Νευτώνειων ρυθμών διάτμησης, για το δείγμα S7.

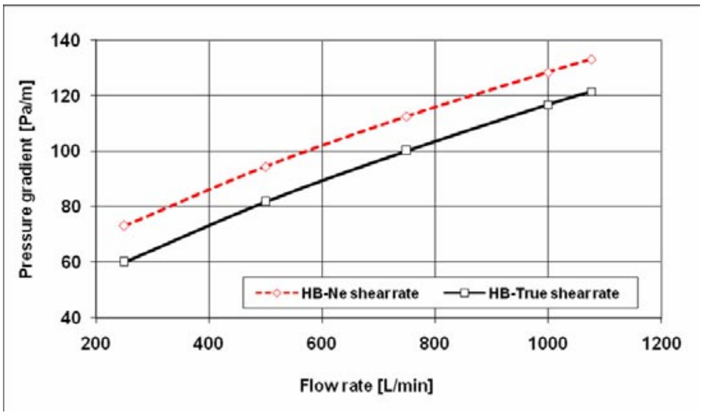

Fig. 10 *Predicted pressure drop gradient in (0.2159 by 0.127 m) annulus in laminar flow regime, for HB model rheological parameters derived by Newtonian and true shear rate for sample S5*

Σχήμα 10. Εκτιμώμενη πτώση πίεσης για δακτύλιο (0.2159 X 0.127 m) σε στρωτή ροή για μοντέλο HB, με χρήση πραγματικών και Νευτώνειων ρυθμών διάτμησης, για το δείγμα S5.

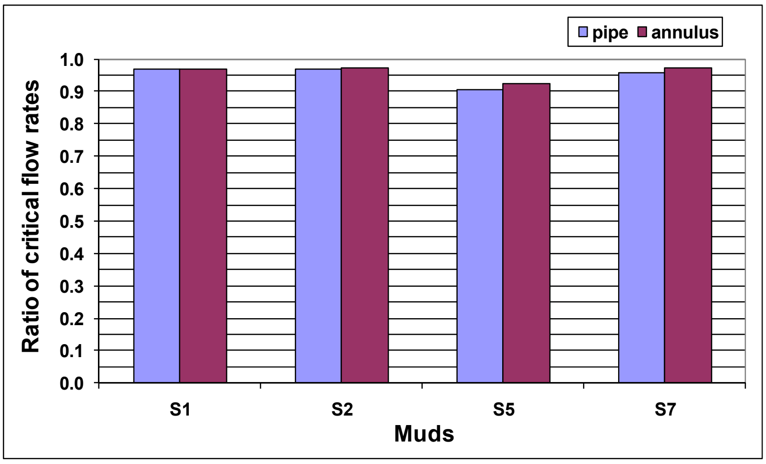

Fig. 11 *Ratio of predicted critical flow rates, true to Newtonian shear rates*

Σχήμα 11. Λόγοι εκτιμώμενων κρισίμων παροχών, πραγματικών προς Νευτώνειων ρυθμών διάτμησης

Vassilios Kelessidis
Mineral Resources Engineering Department, Technical University of Crete, Polytechnic City, 73100 Chania, Greece
Phone: +30 28210 37621, Fax: +30 28210 37874 e-mail: kelesidi@mred.tuc.gr
Roberto Maglione
Consultant, Vercelli, Italy

Extended summary

Επιλογή του Καλύτερου Ρεολογικού Μοντέλου για Αιωρήματα Μπεντονίτη-Νερού

ROBERTO MAGLIONE
Μηχανικός Μεταλλείων και Πετρελαίου

ΒΑΣΙΛΕΙΟΣ ΚΕΛΕΣΙΔΗΣ
Αναπληρωτής Καθηγητής
Τμήμα Μηχανικών Ορυκτών Πόρων

Σύνοψη
Ροή υδατικών αιωρημάτων μπεντονίτη απαντάται συχνά στις βιομηχανίες γεωτρήσεων, χημικές, πετρελαϊκές και διαχείρισης αποβλήτων όπως, επίσης, και σε πολύπλοκες γεωμετρίες όπως ροή σε σωλήνες, σε ομόκεντρο και έκκεντρο δακτύλιο και σε ορθογωνικούς αγωγούς. Τις περισσότερες φορές η ροή είναι στρωτή και έχουν αναπτυχθεί αναλυτικές λύσεις για την πρόβλεψη της πτώσης πίεσης για διάφορα ρεολογικά μοντέλα όπως τα μοντέλα Casson, Robertson-Stiff και Herschel-Bulkley. Ιξωδόμετρα τύπου Couette έχουν χρησιμοποιηθεί για τον προσδιορισμό του κατάλληλου ρεολογικού μοντέλου, αλλά τις περισσότερες φορές οι ρυθμοί διάτμησης προσδιορίζονται ως να είναι τα ρευστά Νευτώνεια ή με τη χρήση της προσέγγισης του στενού διαστήματος, δίδοντας έτσι μόνο κατά προσέγγιση τις τιμές των ρεολογικών παραμέτρων για το συγκεκριμένο μοντέλο. Τελευταίες εξελίξεις επιτρέπουν τον υπολογισμό των πραγματικών ρυθμών διάτμησης για κάθε ένα από τα τρία μοντέλα που αναφέρθηκαν. Με τη χρήση ρεολογικών δεδομένων από τη βιβλιογραφία χρησιμοποιούνται τα τρία μοντέλα για να υπολογιστούν οι ρεολογικές παράμετροι με τη χρήση Νευτώνειων και πραγματικών ρυθμών διάτμησης και εκτιμάται το μοντέλο που περιγράφει καλύτερα τα δεδομένα. Εκτιμώνται ακολούθως οι παράμετροι ροής για στρωτή ροή σε σωλήνες και δακτύλιο, όπως το προφίλ ταχύτητας, η πτώση πίεσης και η μετάβαση σε τυρβώδη ροή. Αναλύονται δε και συζητούνται οι διαφορές στη ρεολογική συμπεριφορά των τριών μοντέλων με τη χρήση ρυθμών διάτμησης Νευτώνειου μοντέλου και των πραγματικών ρυθμών διάτμησης, όπως και οι προβλέψεις για τις παραμέτρους ροής.

1. ΕΙΣΑΓΩΓΗ

Υδατικά αιωρήματα μπεντονίτη χρησιμοποιούνται σε πολλές βιομηχανίες και ιδιαίτερα στη βιομηχανία γεωτρήσεων [5,19-22]. Τα ρεολογικά μοντέλα, που συνδέουν τον ρυθμό διάτμησης με τη διατμητική τάση , είναι το μοντέλο τριών παραμέτρων Herschel-Bulkley [9,14, 15,, 18, 28, 31], που δίδεται από την εξίσωση (1), το επίσης τριών παραμέτρων μοντέλο Robertson-Stiff [3,36] που δίδεται από την εξίσωση (2) και το μοντέλο δύο παραμέτρων Casson [2,6] που δίδεται από την εξίσωση (3).

Υποβλήθηκε: 28.9.2009 Έγινε δεκτή: 26.10.2010

Στη βιομηχανία πετρελαίου τα ρεογράμματα λαμβάνονται με ιξωδόμετρα Couette στενού διακένου 1.170 mm με λόγο διαμέτρων 1.06780 [1,5]. Τα ρεογράμματα () υπολογίζονται με ρυθμούς διάτμησης θεωρώντας ότι τα ρευστά είναι Νευτώνεια, , ενώ, εάν τα ρευστά ακολουθούν ένα των ανωτέρω τριών μοντέλων, οι ρυθμοί διάτμησης θα είναι διαφορετικοί. Οι διαφορές έχουν αναλυθεί με χρήση ακολουθιών [7, 11, 12, 16, 23-26]. Πρόσφατα έχει αποδειχθεί ότι για ρευστά Casson και Robertson-Stiff, οι διαφορές μολονότι μικρές, υπάρχουν και πρέπει να λαμβάνονται υπόψη [19], ενώ για ρευστά Herschel-Bulkley οι διαφορές αυτές είναι ακόμη μεγαλύτερες [22].

Η επιλογή του κατάλληλου ρεολογικού μοντέλου είναι σημαντική για υπολογισμό πτώσης πίεσης, μεταφοράς τριμμάτων, υπολογισμό προφίλ ταχυτήτων [5,17,35] και για τον λόγο αυτό είναι απαραίτητο να μπορούμε να επιλέξουμε το καλύτερο ρεολογικό μοντέλο. Ο σκοπός της εργασίας αυτής είναι να αναλύσει ρεολογικά δεδομένα με χρήση Νευτώνειων και πραγματικών ρυθμών διάτμησης και προσδιορίσει το καλύτερο μοντέλο εκ των τριών με χρήση τριών στατιστικών δεικτών και ακολούθως να προσδιορίσει την επίπτωση με τον υπολογισμό της πτώσης πίεσης και των προφίλ ταχύτητας, με τη χρήση μοντέλων που προτάθηκαν από [10,20].

2. ΘΕΩΡΙΑ

Η διατμητική τάση για Νευτώνειο ρευστό σε ιξωδόμετρο δίδεται από την εξίσωση (4) και ο Νευτώνειος ρυθμός διάτμησης από την εξίσωση (5). Ο πραγματικός ρυθμός διάτμησης για ρευστό Casson δίδεται από την (6) [12,16,19], για ρευστό Robertson-Stiff fluid [19] και για ρευστό Herschel-Bulkley [22] δίδονται $τις εξισώσεις (8) και (9). Για το καθένα από τα μοντέλα μπορεί να υπολογιστεί το άθροισμα των τετραγώνων απόκλισης SSE και η τετραγωνική ρίζα του μέσου σφάλματος $RMSE$ από $ις εξισώσεις (10) και (11).

3. Υλικά και μεθοδολογία

Χρησιμοποιήθηκαν δεδομένα από τέσσερα υδατικά διαλύματα από τη βιβλιογραφία [18], που παρουσιάζονται στον Πίνακα 1. Με χρήση μη γραμμικής παλινδρόμησης υπολογίστηκαν οι ρεολογικές παράμετροι για τα τρία μοντέλα, πρώτα με την υπόθεση των Νευτώνειων ρυθμών διάτμησης και ακολούθως με τη χρήση των πραγματικών ρυθμών διάτμησης. Παράλληλα υπολογίστηκαν οι δείκτες , , και, .

4. Αποτελέσματα και συζήτηση

Στο Σχήμα 1. παρουσιάζονται τα ρεολογικά δεδομένα και το ρεόγραμμα με χρήση Νευτώνειων ρυθμών διάτμησης για το δείγμα S1, ενώ οι ρεολογικές παράμετροι παρουσιάζονται στον Πίνακα 2. Το HB μοντέλο περιγράφει τα δεδομένα καλύτερα σε δύο από τις τέσσερις περιπτώσεις, ενώ για το S5 είναι το Casson και για το S7 το RS μοντέλο, αλλά το HB μοντέλο παρουσιάζει εξίσου καλούς δείκτες.

Στο Σχήμα 2 παρουσιάζονται τα δεδομένα και το ρεόγραμμα με χρήση πραγματικών ρυθμών διάτμησης για το δείγμα S1, ενώ οι ρεολογικές παράμετροι παρουσιάζονται στον Πίνακα 3. Φαίνεται ότι το HB μοντέλο περιγράφει καλύτερα τα δεδομένα για 3 από τις 4 περιπτώσεις (S1, S5 και S7).

Στο Σχήμα 3 παρουσιάζονται οι λόγοι των ρυθμών διάτμησης, Νευτώνειων και πραγματικών για το δείγμα S1, με παρόμοια συμπεριφορά για S2, S5, και S7. Συνεπώς, η υπόθεση ότι οι ρυθμοί διάτμησης είναι Νευτώνειοι δίδουν υψηλότερες τιμές από τις πραγματικές τιμές και για τα τρία μοντέλα.

Η παραπάνω σύγκριση έδειξε ότι το μοντέλο HB βασισμένο στους πραγματικούς ρυθμούς διάτμησης είναι το καλύτερο ρεολογικό μοντέλο. Με τη χρήση αυτών των ρεολογικών παραμέτρων υπολογίστηκαν οι επιδράσεις στις παραμέτρους ροής.

Στα Σχήματα 4 και 5 παρουσιάζονται τα προφίλ ταχύτητας σε σωλήνα (για το δείγμα S1) και δακτύλιο (για το δείγμα S7), αντίστοιχα, για διάφορες παροχές υπολογισμένων με το μοντέλο [18], με χρήση ρεολογικών παραμέτρων με υπόθεση Νευτώνειων και πραγματικών ρυθμών διάτμησης, με αποτέλεσμα μικρές διαφορές στα προφίλ ταχύτητας. Οι Πίνακες 4 και 5 δίδουν τις τιμές ακτίνων, όπου παρουσιάζεται η ροή εμβόλου (plug flow) για τη ροή HB ρευστού με τιμές υπολογισθείσες με την υπόθεση Νευτώνειων και πραγματικών ρυθμών διάτμησης.

Στα Σχήματα 6, 7, 8 παρουσιάζονται τα αποτελέσματα για την πτώση πίεσης για τον σωλήνα για διάφορες παροχές, υπολογισμένων με το μοντέλο [20], για τα δείγματα S1, S5, S7, με χρήση ρεολογικών παραμέτρων με υπόθεση Νευτώνειων και πραγματικών ρυθμών διάτμησης. Χρήση των πραγματικών ρυθμών διάτμησης δίδει τιμές πτώσης πίεσης χαμηλότερες από τη χρήση Νευτώνειων ρυθμών διάτμησης με μέγιστη διαφορά (–8.7%) για το S1, (-7.4%) για το S2, (–19.1%) για το S5 και (-15.9%) για το S7. Επίσης, παρατηρούνται διαφορές στην έναρξη της μεταβατικής ροής με τη μεγαλύτερη διαφορά για το S5.

Στα Σχήματα 9 και 10 παρουσιάζονται τα αποτελέσματα για την πτώση πίεσης για τον δακτύλιο για διάφορες παροχές, για τα δείγματα S7 και S5 με χρήση ρεολογικών παραμέτρων με υπόθεση Νευτώνειων και πραγματικών ρυθμών διάτμησης. Χρήση των πραγματικών ρυθμών διάτμησης δίδει τιμές πτώσης πίεσης χαμηλότερες από τη χρήση Νευτώνειων ρυθμών διάτμησης με μέγιστη διαφορά (–18.0%) για το S5 και (-13.3%) για το S7. Επίσης, παρατηρούνται διαφορές στην έναρξη της μεταβατικής ροής με τη μεγαλύτερη διαφορά για το S5.

Στο Σχήμα 11. παρουσιάζονται οι λόγοι των υπολογισθέντων κρισίμων παροχών για τη μετάβαση στην τυρβώδη ροή σε σωλήνα και δακτύλιο, με χρήση ρεολογικών παραμέτρων εκτιμηθέντων με Νευτώνειους και πραγματικούς ρυθμούς διάτμησης που κυμαίνονται μεταξύ 0.91 και 0.97 με το δείγμα S5 να παρουσιάζει τον μικρότερο λόγο.

5. Συμπεράσματα

Ρεολογικά δεδομένα για υδατικά αιωρήματα μπεντονίτη αναλύθηκαν για τον προσδιορισμό του καλύτερου ρεολογικού μοντέλου μεταξύ των μοντέλων Casson, Robertson-Stiff και Herschel-Bulkley με τη χρήση Νευτώνειων και πραγματικών ρυθμών διάτμησης.

Παρουσιάστηκαν διαφορές ανάμεσα στις ρεολογικές παραμέτρους που υπολογίστηκαν για όλα τα μοντέλα. Το μοντέλο Herschel–Bulkley υπολογισμένο με τη χρήση πραγματικών τιμών ρυθμών διάτμησης έδωσε την καλύτερη περιγραφή, ενώ το μοντέλο Casson έδωσε τη χαμηλότερη ακρίβεια.

Για ροή σε σωλήνα και δακτύλιο με τη χρήση των παραμέτρων για το καλύτερο μοντέλο με Νευτώνειους ή πραγματικούς ρυθμούς διάτμησης εκτιμήθηκαν διαφορές στον υπολογισμό παραμέτρων ροής, που παρουσιάζουν μέγιστο (-19.1%) για την πτώση πίεσης, ενώ βρέθηκαν μικρές διαφορές στα προφίλ ταχύτητας. Παρατηρήθηκαν, επίσης, διαφορές στις κρίσιμες παροχές για μετάβαση σε τυρβώδη ροή, που κυμάνθηκαν μεταξύ (-9.0%) και (-7.0%).

ΑΝΑΦΟΡΕΣ

1. American Petroleum Institute Specifications 13A (1993) Specification for Drilling Fluids Materials
2. Bailey WJ, Weir IS (1998) Investigation of methods for direct rheological model parameter estimation. J Petrol Science and Engineering 21:1-13
3. Beirute RM, Flumerfelt RW (1977) An evaluation of the Robertson-Stiff model describing rheological properties of drilling fluids and cement slurries. Soc Petr Engrs J 17:97-100
4. Bird, RB, Stewart WE and Lightfoot EN (2007) Transport Phenomena (Revised Second Edition ed.). John Wiley & Sons
5. Bourgogne AT, Chenevert ME, Millheim KK, Young FS (1991) Applied Drilling Engineering, vol 2. SPE Textobook Series, Richardson
6. Casson N (1957) A flow equation for pigment-oil dispersions of the printing ink type, in Mill CC (edts) Rheology of disperse systems. Proceedings of the Conference of the British Society of Rheology, University College, Swansea, Pergamon, London
7. Darby R (1985) Couette viscometer data reduction for materials

with a yield stress. J Rheol 29:369-378
8. Dodge DW, Metzner AB (1959) Turbulent flow in non-Newtonian systems. AIChE J. 5:189–204
9. Fordham EJ, Bittleston SH, Tehrani MA (1991) Viscoplastic flow in centered annuli, pipes and slots. I & EC Research 29: 517-524
10. Founargiotakis K, Kelessidis VC, Maglione R (2008) Laminar, turbulent and transitional flows of Herschel-Bulkley fluids in annuli, Can. J. Chem. Eng., 86:676-683.
11. Govier GW, Aziz K (1972) The flow of complex mixtures in pipes. Krieger, Malabar, Florida, USA.
12. Hanks RW (1983) Couette viscometry of Casson fluids. J Rheol 27:1-6.
13. Helland I (1988) On the structure of partial least squares regression. Communications in Statistics-Simulation and Computations 17:581-607
14. Hemphil T, Campos W, Tehrani MA (1993) Yield power law model accurately predicts mud rheology. Oil Gas J. 91, 45–50.
15. Herschel WH, Bulkley R (1926) Konsistenzmessungen von Gummi-Benzollosungen. Kolloid Z 39:291–300.
16. Joye DD (2003) Shear rate and viscosity corrections for a Casson fluid in cylindrical (Couette) geometries. J Colloidal and Interface Sci 267:204-210
17. Kelessidis VC, Bandelis GE (2004) Flow patterns and minimum dispersion velocity for efficient cuttings transport in horizontal and deviated wells in coiled–tubing drilling. SPE Drilling and Completion 19:213-227
18. Kelessidis VC, Mihalakis TS, Tsamantaki C (2005) Rheology and rheological parameter determination of bentonite–water and bentonite–lignite–water mixtures at low and high temperatures. Proceedings 7th World Congress in Chem. Engineering, Glasgow, July 2005.
19. Kelessidis VC, Maglione R (2006) Modeling rheological behavior of bentonite suspensions as Casson and Robertson-Stiff fluids using Newtonian and true shear rates in Couette viscometry, Powder Tech 168, 137-147.
20. Kelessidis VC, Maglione R, Tsamantaki C, Aspirtakis, Y (2006) Optimal determination of rheological parameters for Herschel-Bulkley drilling fluids and impact on pressure drop, velocity profiles and penetration rates during drilling, J. Petr. Science & Eng. 53, 203-224.
21. Kelessidis VC, Tsamantaki C, Dalamarinis P (2007) Effect of pH and electrolyte on the rheology of aqueous Wyoming bentonite dispersions, Appl. Clay Sci, 38, 86–96.
22. Kelessidis VC, Maglione R (2008) Shear rates corrections for Herschel-Bulkley fluids in Couette geometry and effects on frictional loss estimation, Appl. Rheol. 18:3, 34482-1 – 34482-11
23. Krieger IM (1968) Shear rate in the Couette viscometer. Trans Soc Rheology 12:5-11
24. Krieger IM, Maron SH (1952) Direct determination of flow curves of non-Newtonian fluids. J Applied Physics 23:147-149
25. Krieger IM, Elrod H (1953) Direct determination of flow curves of non-Newtonian fluids. J Applied Physics 24:134-137.
26. Krieger IM, Maron SH (1954) Direct determination of the flow curves of non-Newtonian fluids, III Standardized treatment of viscometric data. J Applied Physics 25:72-76.
27. Maglione R, Robotti G (1996) A Numerical Procedure for Solving a N non-Linear Equations Systems for Determining the Three Rheological Parameters of a Drilling Mud from Experimental Data. Proceeding of the Fourth International Conference on Integral Methods in Science and Engineering, pp 144-149.
28. Maglione R, Ferrario G (1996) Equations determine flow states for yield-pseudoplastic drilling fluids. Oil Gas J. 94, 63–66.
29. Maglione R, Romagnoli R (1999) Idraulica dei Fluidi di Perforazione. Edizioni Cusl, Turin (Italy).
30. Maglione R, Guarneri A, Ferrari G (1999) Rheologic and hydraulic parameter integration improves drilling operations. Oil Gas J. 97, 44–48.
31. Maglione R, Robotti G, Romagnoli R (2000) In-situ characterization of drilling mud. SPE Journal 5:377-386.
32. Maglione R., Kelessidis VC (2006), Choosing the best rheological model for bentonite suspensions, Proceedings, 3rd Annual European Rheology Conference, Hersonissos Crete, April 27-29.
33. Mitsoulis E (2007) Flows of Viscoplastic Materials: Models and Computations, Rheology Reviews, London, UK, Brit. Soc. Rheol., 135-178 pages (bookchapter).
34. Patil PD, Ochoa I, Feng JJ and Hatzikiriakos SG (2008), Viscoelastic flow simulation of polytetrafluoroethylene (PTFE) paste extrusion, J Non-Newtonian Fluid Mechanics, 153:25-33
35. Pilehvari AA, Azar JJ, Shirazi SA (1999) State of the art cuttings transport in horizontal wellbores. SPE Dril and Compl 14:196–200
36. Robertson RE, Stiff HA (1976) An improved rheological model for relating shear stress to shear rate in drilling fluids and cement slurries. Soc Pet Engrs J 16:31-36.
37. Van Pham T, Mitsoulis E (1998) Viscoplastic flows in ducts, The Canadian Journal of Chemical Engineering, 76:120–125.

RobertoMaglione
Μηχανικός Μεταλλείων και Πετρελαίου
Βασίλειος Κελεσίδηςs
Αναπληρωτής Καθηγητής, M.Sc. (Oregon State University, USA), Ph.D. (Univ. of Houston, USA)